Ultraviolet Absorption Spectrum of Cyclic S_2O in Solid Ar

Wen-Jui Lo*

Department of Nursing, Tzu Chi College of Technology, 880, Sec. 2, Chien Kuo Road, Hualien 970, Taiwan

Yu-Jong Wu and Yuan-Pern Lee*,†

Department of Chemistry, National Tsing Hua University, 101, Sec. 2, Kuang Fu Road,
Hsinchu 30013, Taiwan

Received: March 4, 2003; In Final Form: May 28, 2003

Disulfur monoxide dispersed in solid Ar at 15 K was irradiated with light at 308 nm from an XeCl excimer laser to form cyclic S_2O, denoted *cyc*-S_2O; *cyc*-S_2O was identified according to infrared absorption lines reported previously. Using a similar technique to produce *cyc*-S_2O, we recorded both infrared and ultraviolet absorption spectra of the same matrix sample before and after photolysis at various stages. A progression recorded in a range 330−370 nm with intervals ~580 cm^{-1} correlates well with variations in intensities of infrared absorption lines of *cyc*-S_2O. On the basis of characteristics of this observed progression and calculations of vertical excitation energy and oscillator strength using the time-dependent density-functional theory, we tentatively assign this progression to an electronic transition $2^1B_1 \leftarrow X\,^1A_1$ of *cyc*-S_2O; the observed progression is associated with the S−S stretching (ν_2) mode in the excited state. The $2\,^1B_1$ state lies ~77.7 kcal mol^{-1} (27 166 cm^{-1}) above the ground electronic state.

1. Introduction

The structures and energies of cyclic isomers of O_3,[1−3] SO_2,[3−5] S_2O,[3,6,7] and S_3[3,8−11] have been studied extensively because of their potential importance in atmospheric or planetary chemistry.

In our previous investigations with infrared (IR) absorption, we observed only SOO but no *cyc*-SO_2 upon laser photolysis of angular OSO isolated in a low-temperature matrix with laser light at 193 nm.[5] In contrast, using a similar technique, we produced *cyc*-CS_2 on irradiation of linear SCS isolated in solid N_2 or Ar at 193 nm; IR absorption lines at 881.3 and 520.9 cm^{-1} were assigned to *cyc*-CS_2 in a N_2 matrix on the basis of isotopic substitution experiments and theoretical calculations.[12] We recorded also an ultraviolet (UV) absorption spectrum of the irradiated matrix sample with two progressions (330−380 nm) of which variations in intensities correlate well with those of IR absorption of *cyc*-CS_2 upon photolysis of linear SCS at various stages using different wavelengths.[13] On the basis of theoretical calculations of electronically excited states of *cyc*-CS_2 and considerations of vibronic symmetry, we tentatively assigned these two progressions as transitions $2\,^1B_2 \leftarrow X\,^1A_1$ and $2\,^1B_1 \leftarrow X\,^1A_1$ of *cyc*-CS_2.

Recently, disulfur monoxide in a cyclic form, denoted *cyc*-S_2O, is produced on irradiation of linear SSO isolated in solid N_2 or Ar at 15 K with laser light at 308 nm; IR absorption lines at 799.1 (797.0), 574.9, and 544.1 (545.6) cm^{-1} were assigned to *cyc*-S_2O isolated in an Ar matrix; numbers in parentheses correspond to absorption of *cyc*-S_2O isolated in a minor matrix site.[14] Conversion of *cyc*-S_2O to SSO is observed upon further irradiation of the matrix sample with laser light at 248 nm. According to theoretical calculations,[3,6,7,14] *cyc*-S_2O has a S−S bond of length ~2.06 Å, two S−O bonds of length ~1.72 Å, with ∠SOS ≅ 73°; both S−S and S−O bonds are elongated relative to those of SSO (~1.89 and ~1.48 Å, respectively). Although *cyc*-S_2O lies ~41 kcal mol^{-1} above SSO, once formed it is metastable. An asymmetric transition state connecting SSO and *cyc*-S_2O yields a barrier for isomerization ~122 kcal mol^{-1}.[14]

Similarly to work on *cyc*-CS_2, we recorded both UV and IR spectra of an Ar matrix sample containing SSO after various stages of photolysis and identified a UV absorption spectrum in a region 330−370 nm that correlates well with IR absorption of *cyc*-S_2O. We tentatively assign this UV spectrum as the electronic transition $2\,^1B_1 \leftarrow X\,^1A_1$ of *cyc*-S_2O.

2. Experiments

The experimental setup is similar to that described previously.[14−16] The matrix support was a platinum-plated copper mirror maintained at 15 K with a closed-cycle refrigerator. Matrix samples were prepared on depositing gas mixtures of SSO and Ar onto the cold support. Typically, ~10 mmol of mixture was deposited over a period of 3 h. A small proportion of SSO was converted to *cyc*-S_2O on irradiation of the matrix with light from a XeCl excimer laser at 308 nm (~4 mJ per pulse, 30 Hz) for 2 h. Secondary photolysis of the sample was performed with a KrF excimer laser at 248 nm (~3 mJ per pulse, 30 Hz). The system is designed so that IR and UV absorption spectra of the same matrix sample can be recorded consecutively with a Fourier transform spectrometer (Bomem DA8.3). IR absorption spectra were recorded with a globar source, a KBr beam splitter, and a HgCdTe detector (77 K), whereas UV absorption spectra covering a spectral range 300−500 nm were recorded with a deuterium lamp, a quartz beam splitter, and a photomultiplier. Typically, 600 scans were collected for IR

---

* Corresponding authors. E-mail: (W.-J. Lo) wjl@tccn.edu.tw; (Y.-P. Lee) yplee@mx.nthu.edu.tw.

† Jointly appointed by the Institute of Atomic and Molecular Sciences, Academia Sinica, Taipei, Taiwan.

10.1021/jp034563j CCC: $25.00

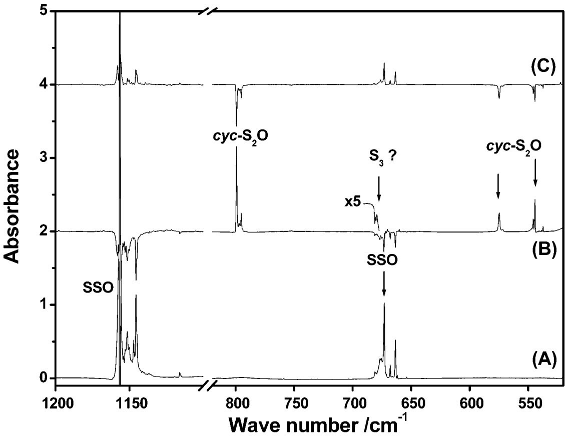

Figure 1. Partial IR absorption spectrum of a matrix sample of SSO/Ar (<1/1000) recorded before irradiation (A), a difference spectrum recorded after irradiation at 308 nm for 2 h (B), and a difference spectrum (relative to trace B) after further irradiation at 248 nm for 0.5 h (C).

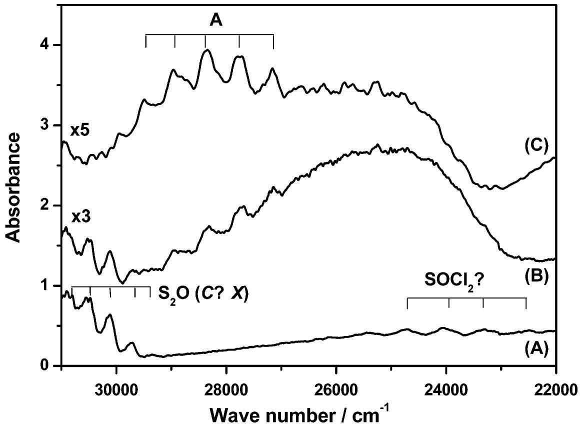

Figure 2. UV absorption spectra of a matrix sample of SSO/Ar (<1/1000) recorded before irradiation (A), after irradiation at 308 nm for 2 h (B), and an inverse difference spectrum after further irradiation at 248 nm for 0.5 h (C); see text.

measurements at a resolution of 0.5 cm^{-1}, and 2000 scans were collected for UV measurements at a resolution of 2.0 cm^{-1}.

SSO was prepared by passing a mixture of $SOCl_2$ and Ar through a tube containing Ag_2S powder prior to deposition.[17] The molar fraction of $SOCl_2$ in Ar was typically 1/1000. $SOCl_2$ (>99%, Fluka Chemika) and Ag_2S (99.0%, Showa Chemicals) were used without further purification, except for degassing at 77 K.

3. Results and Discussion

3.1. IR Absorption Spectra of SSO and *cyc*-S_2O. In Figure 1, trace A shows a partial IR absorption spectrum of SSO isolated in solid Ar (SSO/Ar < 1/1000) after deposition. Intense lines at 1157.6 and 672.5 cm^{-1} are assigned to the S−O stretching (ν_1) and the S−S stretching (ν_3) modes of SSO, respectively.[18] Lines at 1355.5 (1351.2), 1145.6, and 519.4 (517.2) cm^{-1}, not shown in Figure 1, are due to SO_2, respectively.[19] Trace B of Figure 1 shows a difference spectrum recorded after irradiation of the matrix sample at 308 nm for 2 h; a positive feature indicates production after irradiation, whereas a negative feature indicates destruction. New lines that appeared at 799.1 (797.0), 574.9, and 544.1 (545.6) cm^{-1} are assigned to ν_1 (S−O symmetric stretching), ν_3 (S−O asymmetric stretching), and ν_2 (S−S stretching) modes of *cyc*-S_2O, respectively; wavenumbers listed in parentheses are associated with species in a minor matrix site.[14] Lines attributed to SSO decreased, and those attributed to SO_2 increased slightly. A weak line at 680.9 cm^{-1} might be attributable to S_3.[20]

Further irradiation of the matrix sample with laser light at 248 nm for 0.5 h diminished lines of *cyc*-S_2O, whereas lines due to SSO and SO_2 became enhanced, as illustrated in the difference spectrum (relative to trace B) in trace C of Figure 1.

3.2. UV Absorption Spectra. UV absorption spectra were recorded immediately after IR spectra were recorded at each stage of laser irradiation. In Trace A of Figure 2, absorption features in the range 29000−31000 cm^{-1} with lines at 29309, 29712, 30102, 30490, and 30826 cm^{-1} are readily assigned to SSO; the first band observed at 29309 cm^{-1} and intervals ~400 cm^{-1} are close to values ν_{00} = 29687.72 cm^{-1} and ν_3' (S−S stretching) = 410.6 cm^{-1} reported for the $C\ ^1A' \leftarrow X\ ^1A'$ transition of gaseous SSO.[21−25] A similar spectrum of SSO isolated in solid Xe has been reported with ν_{00} = 29285 cm^{-1} and ν_3 = 415 cm^{-1}.[26] Weak absorption features in the range from 22000 to 28000 cm^{-1} with lines at 22505, 23314, 24060, 24745, and 25451 cm^{-1} are likely assignable to the $B\ ^1B_2 \leftarrow X\ ^1A_1$ transition of $SOCl_2$. To our knowledge, there is no experimental report on this transition; the first intense absorption is a continuum near 290 nm.[27] According to our calculations using time-dependent density functional theory (TD-DFT) with a B3LYP/aug-cc-pVTZ basis set, the transition $B\ ^1B_2 \leftarrow X\ ^1A_1$ has a vertical excitation energy ~2.85 eV (~22960 cm^{-1}) with an oscillator strength of 0.01.

TABLE 1: Observed UV Absorption Features Attributed to *cyc*-S_2O in Solid Ar

wavelength /nm	wavenumber /cm^{-1}	interval /cm^{-1}
368.11	27166	
360.41	27746	580
353.04	28325	579
346.02	28900	575
339.33	29470	570

In Trace B of Figure 2, recorded after irradiation of the sample at 308 nm for 2 h, a new absorption band structure with intervals ~580 cm^{-1}, designated as progression A, in a region 330−370 nm (27000−30000 cm^{-1}) lying on top of an extremely broad new feature in a region 345−435 nm (23000−29000 cm^{-1}) appeared. The latter might be assigned to absorption of S_3.[20] S_3 and SO_2 might be produced via bimolecular reaction between two adjacent SSO molecules,[17] consistent with results of IR absorption in which lines attributable to SO_2 and S_3 were observed after irradiation of the matrix sample at 308 nm. We detect no absorption of the $a\ ^3B_1 \leftarrow X\ ^1A_1$ system of SO_2, for which ν_{00} = 25747 cm^{-1} in solid Ar,[28] presumably because of its small intensity.

After secondary photolysis at 248 nm of the sample for 0.5 h, lines belonging to progression A diminished but absorption of SSO increased. An expanded difference UV absorption spectrum is shown in Trace C of Figure 2; for convenience of viewing progression A, we plot the trace as Trace B subtracting the spectrum recorded after secondary photolysis. Wavenumbers of observed lines, 27166, 27746, 28325, 28900, and 29470 cm^{-1}, are listed in Table 1; uncertainties are estimated to be ±10 cm^{-1} due to broad width (~250 cm^{-1}). For these reasons and because of expected small isotopic shifts, unambiguous vibronic analysis of this spectrum using ^{18}O- or ^{34}S-isotopic labeling is not feasible.

3.3. Quantum-Chemical Calculations Using TD-DFT. For calculations performed with the Gaussian 98 program,[29] we employed time-dependent density functional theory (TD-DFT)[30−32] to calculate vertical excitation energies of low-lying

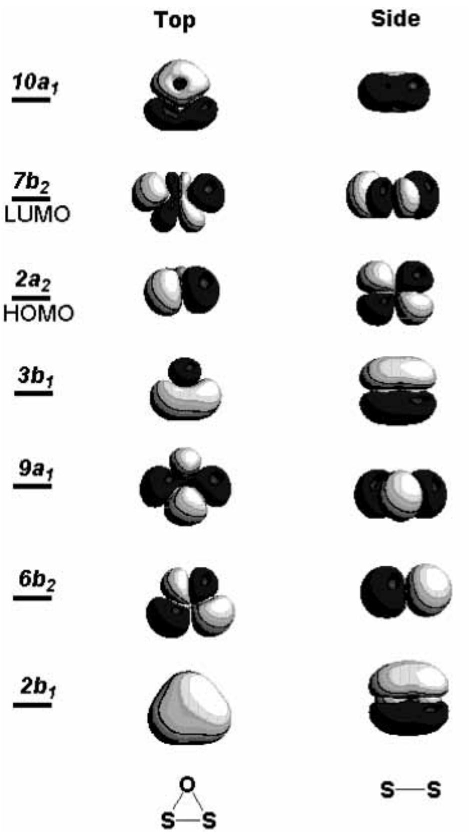

Figure 3. Representative molecular orbitals of *cyc*-S_2O including two unoccupied orbitals.

electronic states of *cyc*-S_2O. The geometry of the ground state $X\ {}^1A_1$, maintaining C_{2v} symmetry, is optimized with the B3LYP method; this method uses Becke's three-parameter hybrid exchange functional,[33] which includes the Slater exchange functional with corrections involving a gradient of the density, and a correlation functional of Lee, Yang, and Parr, with both local and nonlocal terms.[34]

The geometry, energy, and vibrational wavenumbers of *cyc*-S_2O in its ground $X\ {}^1A_1$ state have been characterized theoretically;[3,6,7,14] predicted bond angles ∠SOS in a range 72.4−74.5° are consistent with the experimental bond angle of 72.5 ± 3.0° based on observed isotopic ratios for S−O symmetric and asymmetric stretching modes of *cyc*-S_2O.[14] We calculated vertical excitation energies and oscillator strengths of the first 10 singlet electronic transitions of *cyc*-S_2O from its ground electronic state, using basis sets of two types: aug-cc-pVTZ and aug-cc-pV5Z (representing Dunning's correlation-consistent polarized valence triple-ζ and penta-ζ basis sets, respectively).[35−37] The geometry of the ground electronic state optimized with B3LYP/aug-cc-pVTZ has lengths of 2.058 and 1.724 Å for S−S and S−O bonds, and ∠SOS ≅ 73.3°; predictions based on B3LYP/aug-cc-pV5Z yield lengths of 2.045 and 1.713 Å for S−S and S−O bonds, and a bond angle ∠SOS ≅73.3°.

We assume for the ground state of *cyc*-S_2O an electronic configuration

$$[\text{inner shell}]\ (6a_1)^2\,(7a_1)^2\,(5b_2)^2\,(8a_1)^2\,(2b_1)^2\,(6b_2)^2\,(9a_1)^2\,(3b_1)^2\,(2a_2)^2 \qquad (1)$$

Representative molecular orbitals of *cyc*-S_2O including two unoccupied ones are shown in Figure 3; delocalized three-center bonding is clearly illustrated. The $2b_1$ orbital is a bonding π orbital delocalized throughout the cyclic skeleton. The highest occupied molecular orbital (HOMO), $2a_2$, is described approximately as an antibonding π orbital along the S−S bond, whereas the orbital with slightly less energy ($3b_1$) is described approximately as a π orbital bonding to the S−S bond but antibonding to the S−O bond. The lowest unoccupied molecular orbital (LUMO), $7b_2$, has antibonding σ^* character based on linear combination of three in-plane *p* orbitals.

TABLE 2: Comparison of Vertical Excitation Wave Numbers (cm^{-1}) and Oscillator Strength *f* (listed parenthetically) of *cyc*-S_2O Predicted with Various Theoretical Methds

state	excitation[a]	MRD-CI[b]/ cm^{-1}	TD-DFT/ aug-cc-pVTZ/ cm^{-1}	TD-DFT/ aug-cc-pV5Z/ cm^{-1}	expt[c]/ cm^{-1}
$1\ {}^1B_1$	$2a_2 \rightarrow 7b_2$	20972	17096 (0.0007)	16859 (0.0006)	
$1\ {}^1A_2$	$3b_1 \rightarrow 7b_2$ ($2a_2 \rightarrow 10a_1$)	23472	21329 (0.0000)	21089 (0.0000)	
$2\ {}^1A_2$	$2a_2 \rightarrow 10a_1$ ($3b_1 \rightarrow 7b_2$)	28554	23015 (0.0000)	22686 (0.0000)	
$2\ {}^1B_1$	$3b_1 \rightarrow 10a_1$	31619	26611 (0.0012)	26300 (0.0011)	28 325
$3\ {}^1B_1$	$2a_2 \rightarrow 8b_2$		41152 (0.0062)	41004 (0.0061)	
$3\ {}^1A_2$	$3b_1 \rightarrow 8b_2$		44295 (0.0000)	44258 (0.0000)	
$4\ {}^1A_2$	$2a_2 \rightarrow 11a_1$		50834 (0.0000)	48447 (0.0000)	
$2\ {}^1A_1$	$9a_1 \rightarrow 10a_1$	38878	51501 (0.0038)	51041 (0.0036)	
$1\ {}^1B_2$	$9a_1 \rightarrow 7b_2$ ($6b_2 \rightarrow 10a_1$)	47589	52698 (0.1204)	52238 (0.1213)	
$4\ {}^1B_1$	$3b_1 \rightarrow 11a_1$ ($2a_2 \rightarrow 9b_2$)		56148 (0.0861)	53792 (0.0705)	

[a] Approximate description of orbitals; orbitals showing substantial mixing are included in parentheses. [b] Using [5s3p1d] and [4s2p1d] basis sets for S and O atoms; see ref 6. [c] The most intense band in the progression is listed; the origin of the transition lies at or below 27166 cm^{-1}.

Wavenumbers, oscillator strengths, and representative description of vertical excitation for the first 10 singlet transitions are listed in Table 2 and compared with previous calculations using multireference double-excitation configuration interaction (MRD-CI) with a smaller basis set.[6] Extending the basis set from aug-cc-pVTZ to aug-cc-pV5Z decreases the energy only slightly, indicating that the basis sets are adequate to describe these excited states. The order of energies of the first four excited states is consistent in all calculations, but our excitation energies are believed to be more reliable than the larger energies predicted with MRD-CI using a smaller basis set.[6] The first three transitions with nonnegligible oscillator strength are $1\ {}^1B_1 \leftarrow X\ {}^1A_1$, $2\ {}^1B_1 \leftarrow X\ {}^1A_1$, and $3\ {}^1B_1 \leftarrow X\ {}^1A_1$ with vertical excitation energies predicted to be ~17000, 26500, and 41100 cm^{-1}, and oscillator strengths of 0.0006, 0.0011, and 0.0061, respectively.

3.4. Assignments of Progression A. Whether the first observed member of progression A, lying at 27166 cm^{-1}, is the origin of an electronic transition is unclear because its intensity is small. Intervals in this progression ranging from 570 to 580 cm^{-1} are similar to ν_2 (544.1 cm^{-1}, S−S stretching) and ν_3 (574.9 cm^{-1}, S−O asymmetric stretching) modes of *cyc*-S_2O in its ground electronic state $X\ {}^1A_1$. The photolytic behavior of lines in this progression correlates well with that of IR absorption lines of *cyc*-S_2O. Considering possible photolysis products of SSO in solid Ar and observed IR absorption spectra, we tentatively assign progression A to *cyc*-S_2O.

According to calculations with B3LYP/aug-cc-pV5Z, vertical excitations to the first four excited singlet states, $1\ {}^1B_1$, $1\ {}^1A_2$, *2* $^1A_2$, and *2* $^1B_1$, of *cyc*-S_2O lie ∼16859, 21089, 22686, and 26300 cm^{-1} above the ground *X* $^1A_1$ state, respectively; excitation to the fifth excited singlet state, *3* $^1B_1$, requires more than 5 eV (above 40300 cm^{-1}). In view of possible errors in calculations, observed new transitions near 27166 cm^{-1} correlate well with a transition to the fourth excited state *2* $^1B_1$, predicted to have a vertical excitation energy ∼26300 cm^{-1}. Transitions to the two lower states *1* $^1A_2$ and *2* $^1A_2$ are forbidden by symmetry, consistent with the zero oscillator strength calculated for these two transitions (Table 2).

The TD-DFT method allows no prediction of vibrational wavenumbers for an electronically excited state. According to vibronic symmetry of C_{2v} molecules, only ν_1 and ν_2 modes of A_1 symmetry are allowed for the transition $^1B_1 \leftarrow {}^1A_1$. Considering the observed separation of bands and expected vibrational wavenumbers, *we tentatively assign progression A as the 2* $^1B_1$ *(0, v, 0)* ← *X* $^1A_1$ *(0, 0, 0) transition*, in which the numbers in parentheses indicate quantum numbers of three vibrational modes; the active ν_2 mode (∼580 cm^{-1}) corresponds to S−S stretching motion (544 cm^{-1} in the *X* $^1A_1$ state). Greater widths for the third and fourth members of the progression indicate a possible second vibrational progression associated with ν_1, the symmetrical S−O stretching mode with a vibrational wavenumber of 799 cm^{-1} in the *X* $^1A_1$ state. That the ν_2 vibrational wavenumber is greater in the excited state is consistent with calculations for the transition 2 $^1B_1$ ← X $^1A_1$ in which a bonding π orbital is excited to a bonding σ orbital of the S−S bond.

4. Conclusion

We have recorded a new UV absorption spectrum in a spectral region 330−370 nm after irradiation of an Ar matrix containing SSO with laser light at 308 nm. These spectral features show photolytic behavior correlating with IR absorption lines of *cyc*-S_2O at 799.1 (797.0), 574.9, and 544.1 (545.6) cm^{-1}; they appear upon irradiation of SSO at 308 nm and diminish after further irradiation at 248 nm. Based on the correlation of photolytic behavior between the new UV spectrum and the IR absorption spectrum of *cyc*-S_2O, as well as theoretical calculations of vertical excitations of *cyc*-S_2O, we tentatively assign the new progression, with origin lying at or below 27166 cm^{-1}, to the *2* $^1B_1$ ← *X* $^1A_1$ transition of *cyc*-S_2O; observed intervals ∼580 cm^{-1} correspond to the ν_2 (S−S stretching) mode of the upper state.

Acknowledgment. We thank the National Science Council of Taiwan (Grant No. NSC 91-2119-M-007-003) and the MOE Program for Promoting Academic Excellence of Universities (Grant No. 89-FA04-AA) for support.

References and Notes

(1) Meredith, C.; Quelch, G. E.; Schaefer, H. F. *J. Am. Chem. Soc.* **1991**, *113*, 1186.
(2) Lee, T. J. *Chem. Phys. Lett.* **1990**, *169*, 529.
(3) Ivanic, J.; Atchity, G. J.; Ruedenberg, K. *J. Chem. Phys.* **1997**, *107*, 4307.
(4) Kellogg, C. B.; Schaefer, H. F. *J. Chem. Phys.* **1995**, *102*, 4177.
(5) Chen, L.-S.; Lee, C.-I; Lee, Y.-P. *J. Chem. Phys.* **1996**, *105*, 9454.
(6) Fueno, T.; Buenker, R. J. *Theor. Chim. Acta* **1988**, *73*, 123.
(7) Jones, R. O. *Chem. Phys. Lett.* **1986**, *125*, 221.
(8) Jones, R. O. *J. Chem. Phys.* **1986**, *84*, 318.
(9) Rice, J. E.; Amos, R. D.; Handy, N. C.; Lee, T. J.; Schaefer, H. F., III. *J. Chem. Phys.* **1986**, *85*, 963.
(10) Koch, W.; Natterer, J.; Heinemann, C. *J. Chem. Phys.* **1995**, *102*, 6159.
(11) Patterson, C. H.; Messmer, R. P. *J. Am. Chem. Soc.* **1990**, *112*, 4138.
(12) Bahou, M.; Lee, Y.-C.; Lee, Y.-P. *J. Am. Chem. Soc.* **2000**, *122*, 661.
(13) Lo, W.-J.; Lee, Y.-P. *Chem. Phys. Lett.* **2001**, *336*, 71.
(14) Lo, W.-J.; Wu, Y.-J.; Lee, Y.-P. *J. Chem. Phys.* **2002**, *117*, 6655.
(15) Liu, C.-P.; Lai, L.-H.; Lee, Y.-Y.; Hung, S.-C.; Lee, Y.-P. *J. Chem. Phys.* **1998**, *109*, 978.
(16) Lee, Y.-C.; Lee, Y.-P. *J. Phys. Chem. A* **2000**, *104*, 6951.
(17) Tang, S.-Y.; Brown, C. W. *Inorg. Chem.* **1975**, *14*, 2856.
(18) Hopkins, A. G.; Daly, F. P.; Brown, C. W. *J. Phys. Chem.* **1975**, *79*, 1849.
(19) Maillard, D.; Allavena, M.; Perchard, J. P. *Spectrochim. Acta* **1975**, *31A*, 1523.
(20) Hassanazadeh, P.; Andrews, L. *J. Phys. Chem.* **1992**, *96*, 6579.
(21) Lakshminarayana, G. *J. Mol. Spectrosc.* **1975**, *55*, 141.
(22) Hallin, K.-E. J.; Merer, A. J.; Milton, D. J. *Can. J. Phys.* **1977**, *55*, 1858.
(23) Tsukiyama, K.; Kobayashi, D.; Obi, K.; Tanaka, I. *Chem. Phys.* **1984**, *84*, 337.
(24) Clouthier, D. J.; Rutherford, M. L. *Chem. Phys.* **1988**, *127*, 189.
(25) Muller, T.; Vaccaro, P. H.; Perez-Bernal, F.; Iachello, F. *J. Chem. Phys.* **1999**, *111*, 5038.
(26) Phillips, L. F.; Smith, J. J.; Meyer, B. *J. Mol. Spectrosc.* **1969**, *29*, 230.
(27) Donovan, R. J.; Husain, D.; Jackson, P. T. *Trans. Faraday Soc.* **1969**, *65*, 2930.
(28) Zen, C.-C.; Chen, I.-C; Lee, Y.-P.; Merer, A. J. *J. Phys. Chem. A* **2000**, *104*, 771.
(29) Frisch, M. J.; Trucks, G. W.; Schlegel, H. B.; Scuseria, G. E.; Robb, M. A.; Cheeseman, J. R.; Zakrzewski, V. G.; Montgomery, J. A., Jr.; Stratmann, R. E.; Burant, J. C.; Dapprich, S.; Millam, J. M.; Daniels, A. D.; Kudin, K. N.; Strain, M. C.; Farkas, O.; Tomasi, J.; Barone, V.; Cossi, M.; Cammi, R.; Mennucci, B.; Pomelli, C.; Adamo, C.; Clifford, S.; Ochterski, J.; Petersson, G. A.; Ayala, P. Y.; Cui, Q.; Morokuma, K.; Malick, D. K.; Rabuck, A. D.; Raghavachari, K.; Foresman, J. B.; Cioslowski, J.; Ortiz, J. V.; Stefanov, B. B.; Liu, G.; Liashenko, A.; Piskorz, P.; Komaromi, I.; Gomperts, R.; Martin, R. L.; Fox, D. J.; Keith, T.; Al-Laham, M. A.; Peng, C. Y.; Nanayakkara, A.; Gonzalez, C.; Challacombe, M.; Gill, P. M. W.; Johnson, B.; Chen, W.; Wong, M. W.; Andres, J. L.; Gonzalez, C.; Head-Gordon, M.; Replogle, E. S.; Pople, J. A. *Gaussian 98*, revision A.6; Gaussian, Inc.: Pittsburgh, PA, 1998.
(30) Bauernschmitt, R.; Ahlrichs, R. *Chem. Phys. Lett.* **1996**, *256*, 454.
(31) Casida, M. E.; Jamorski, C.; Casida, K. C.; Salahub, D. R. *J. Chem. Phys.* **1998**, *108*, 4439.
(32) Stratmann, R. E.; Scuseria, G. E.; Frisch, M. J. *J. Chem. Phys.* **1998**, *109*, 8218.
(33) Becke, A. D. *J. Chem. Phys.* **1993**, *98*, 5648.
(34) Lee, C.; Yang, W.; Parr, R. G. *Phys. Rev. B* **1988**, *37*, 785.
(35) Peterson, K. A.; Woon, D. E.; Dunning, T. H., Jr. *J. Chem. Phys.* **1994**, *100*, 7410.
(36) Dunning, T. H., Jr. *J. Chem. Phys.* **1989**, *90*, 1007.
(37) Davidson, E. R. *Chem. Phys. Lett.* **1996**, *260*, 514.